Journal of Luminescence 175 (2016) 243–248

Contents lists available at ScienceDirect

Journal of Luminescence

journal homepage: www.elsevier.com/locate/jlumin

Effect of pH on the optical and structural properties of HfO_2:Ln^{3+}, synthesized by hydrothermal route

E. Montes [a,*], I. Martínez-Merlín [a], J.C. Guzmán-Olguín [a], J. Guzmán-Mendoza [a], I.R. Martín [b], M. García-Hipólito [c], C. Falcony [d]

[a] Centro de Investigación en Ciencia Aplicada y Tecnología Avanzada IPN, Legaría 694, 11500, D.F., Mexico
[b] Depto. de Física Fundamental y Experimental, Electrónica y Sistemas, Univ. de La Laguna, Av. Astrofísico Francisco Sánchez s/n E-38206, La Laguna. Tenerife, Spain
[c] Instituto de Investigaciones en Materiales, Universidad Nacional Autónoma de México, Circuito Exterior, Cd. Universitaria, 04510, D.F., Mexico
[d] Departamento de Física, CINVESTAV IPN, Apartado Postal 14-740, 07000, D.F., Mexico

ARTICLE INFO

Article history:
Received 16 December 2015
Received in revised form
6 March 2016
Accepted 8 March 2016
Available online 14 March 2016

Keywords:
Photoluminescence
Hafnium oxide
Hydrothermal synthesis

ABSTRACT

In this work, the influence of the chlorine ions in the optical and structural properties of hafnium oxide (HfO_2) doped with europium (Eu^{3+}) and terbium (Tb^{3+}) are reported. The synthesis was conducted by hydrothermal route at a temperature of 200 °C, with a reaction time of 80 min and a concentration of 3 mol% of both dopants, in relation to hafnium in solution. In order to study the influence of acidity on the kinetics of reaction, the pH of the precursor solution was varied in the range of pH=4 to pH=12. X-ray powder diffraction patterns showed that the materials crystallized better under alkaline conditions with pH=11, noting a better crystallinity in the material doped with Eu^{3+}showed a better crystallinity that Tb^{3+} ions. The characteristic rhombohedral microstructure of HfO_2 in the monoclinic phase was observed in alkaline media. Photoluminescent spectra showed the characteristic peaks of the emissions for both Eu an Tb dopants, where the intensity of the luminescent emission increases by decreasing the concentration of chlorine ions. On the other hand, it was found that radiative life kinetics of the dopant is related to the kinetics of crystallization, and therefore, to the acidity of the precursor solution.

1. Introduction

In the last decades, the development of the different technological areas is closely related to the design and production of new materials. Among these, the luminescent materials have aroused great interest, due to the great breadth of potential applications, the most important include the development of scintillators materials [1], lamps of high efficiency lighting emitting white, as well as different types of luminescent flat screen [2], light emitting diodes (LEDs) [3], dosimetry materials to the UV region [4], likewise in materials for imaging diagnosis of high resolution [5] and molecular markers [6], among others. One of the groups of materials which have attracted more interest are those based on metal oxides, due to the physicochemical properties that possess, as its wide band gap and low phononic frequencies [7]. Among them, the hafnium oxide (HfO_2) is an excellent candidate for its optical properties such as a high index of refraction and hardness, the tetragonal phase is comparable with diamond [8], additionally a high density of about 10 g/cm^3. The high density and atomic numbers of its components made of HfO_2 an excellent candidate as scintillator material [1] even in the detection of X-rays and gamma radiation [9]. Depending on the temperature of synthesis, hafnium oxide presents several polymorphs. Thermodynamically, the more stable phase at room conditions is the monoclinic ($P2_1/C$), while the tetragonal ($P4_2/nmc$) and cubic ($Fm3m$) phases stabilize at temperatures above 1700–2700 °C, respectively [10,11]. The wide band gap of the HfO_2 (~5.68 eV) and low phonon frequencies makes it transparent in a extensive range of the electromagnetic spectrum, from ultraviolet to mid-infrared and appropriate to be doped with lanthanides ions (Ln^{3+}) [12,13]. One of the most important properties of the compounds doped with Ln^{3+} ions is the narrow bands of emission and absorption, due to the intraconfigurational transitions 4f→4f; resulting that the doped materials with Ln^{3+} ions possess a high purity of color [4]. The Eu^{3+} is a trivalent ion that presents emission bands centered in 580 nm, 592 nm, 612 nm, 656 nm and 701 nm, which correspond to the transitions $^5D_0 \rightarrow {}^7F_J$. ($J$=0–4), while trivalent ion Tb^{3+} has emission bands centered in 489 nm, 543 nm, 584 nm and 622 nm, which corresponding to the transitions $^5D_4 \rightarrow {}^7F_J$ (J=3–6) [14].

There are various methods of synthesis for the production of nanostructured metal oxides, which include chemical synthesis,

* Corresponding author.
E-mail address: emontesr@live.com.mx (E. Montes).

http://dx.doi.org/10.1016/j.jlumin.2016.03.009
0022-2313/

sol–gel, co-precipitation, the solvothermal route, among others. The hydrothermal route is an efficient and economic method allowing to control the morphology, size and crystalline phase of particles by adjusting parameters such as temperature, pressure, processing time, concentration and acidity (pH) of the precursor solutions [15]. This last parameter is of particular interest, because many reports indicate that there is a close relationship between the acidity of the precursor solution and kinetics of crystallinity of the HfO_2 [10,16]. Given that, different methodologies for the synthesis of luminescent materials have been focused on the use of metal salts as precursors; the inclusion of chlorine ions within the matrix is almost inevitable. The modification of some optical properties, has been reported when the chlorine ions are incorporated into the matrix, for example, the emergence of new lines of emission [17], or the increase in the intensity of emission luminescent [18,19]. However, the role played within the luminescent emission has not been widely studied. This work focuses on the effect of the acidity of precursor solutions and the addition of chloride ions in the optical and structural properties of the HfO_2 doped with Tb^{3+} and Eu^{3+} ions.

2. Experimental procedure

The synthesis of the HfO_2 doped with Ln^{3+} ions (Tb^{3+}, Eu^{3+}), was conducted by hydrothermal route [15,16]. An aqueous solution $HfCl_4$ 0.04 M (Alfa Aesar 99.9%) was elaborated using deionized water as a solvent; aliquots of 10 ml were taken for each sample. Also prepared solutions of $XCl_3 \cdot 6H_2O$ (X=Tb, Eu) to 0.008 M were elaborated; taken aliquot of 3 ml, which were added to each sample in order to have a 3 mol% of the dopant regarding the hafnium concentration in solution. Later 8 ml of deionized water were added to obtain a final volume of 20 ml. To adjust the acidity of the precursor solution in the interval of pH=4 to pH=12, a 2 M solution of NaOH was used, which was added drop by drop [4,15]. From an acidity of pH=5, was observed the formation of a white precipitate; this suspension remained under constant stirring for 15 min and was subsequently introduced in an ultrasonic bath for 15 min. Immediately after was placed on a teflon container, inside of stainless steel autoclave with capacity of 30 ml, and subjected to hydrothermal treatment at temperature of 200 °C, under autogenous pressure with a reaction time of 80 min. The powder obtained was washed with deionized water and dried at room temperature for 24 h [4]. The structural analysis was carried by X-ray diffraction (XRD) using a diffractometer D8-Advance-Bruker, with a wavelength of radiation of 1.5406 Å (Cu Kα), steps of 0.05° and 0.5 s per step. The morphology of synthesized material was analyzed by mean of a ZEISS SUPRA 55VP, field emission scanning electron microscope (FESEM), using the secondary electrons detector. The elements present in the samples were determined by energy dispersive spectroscopy (EDS) using a silicon–lithium X-ray detector brand Oxford model Pentafet. Radiative mean lifetimes were obtained by fluorescence microscopy using a tunable laser EKSPLA NT-342/2/UVE with 27 mJ power as excitation source. Finally, the spectra of emission Photoluminescence (PL), were obtained using a spectrofluorimeter Flouro Max-P Jobin Yvon Horiba, with a continuous emission of 150 W xenon lamp. All characterization experiments were conducted at room temperature.

3. Results and analysis

Fig. 1 shows the X-ray diffraction patterns of (a) HfO_2:Tb^{3+} and (b) HfO_2:Eu^{3+}, as a function of the pH in the precursor solution. The XRD analysis shows that in both cases an amorphous phase is obtained, for alkalinity values less of pH=10. However, for alkalinity higher values, it is possible to observe that, in addition to the amorphous phase, appear the diffraction peaks of monoclinic phase of hafnium oxide (PDF-34-0104). At values higher than pH=11, both materials exhibit diffraction peaks of the monoclinic phase, however, the HfO_2:Tb^{3+} presents diffraction peaks wider, indicating a lower crystal size with respect to HfO_2:Eu^{3+}. From the diffraction pattern of HfO_2:Tb^{3+}(Fig. 1a) was possible to estimate the size of crystals by means of the Scherrer equation [20], obtaining an approximate value

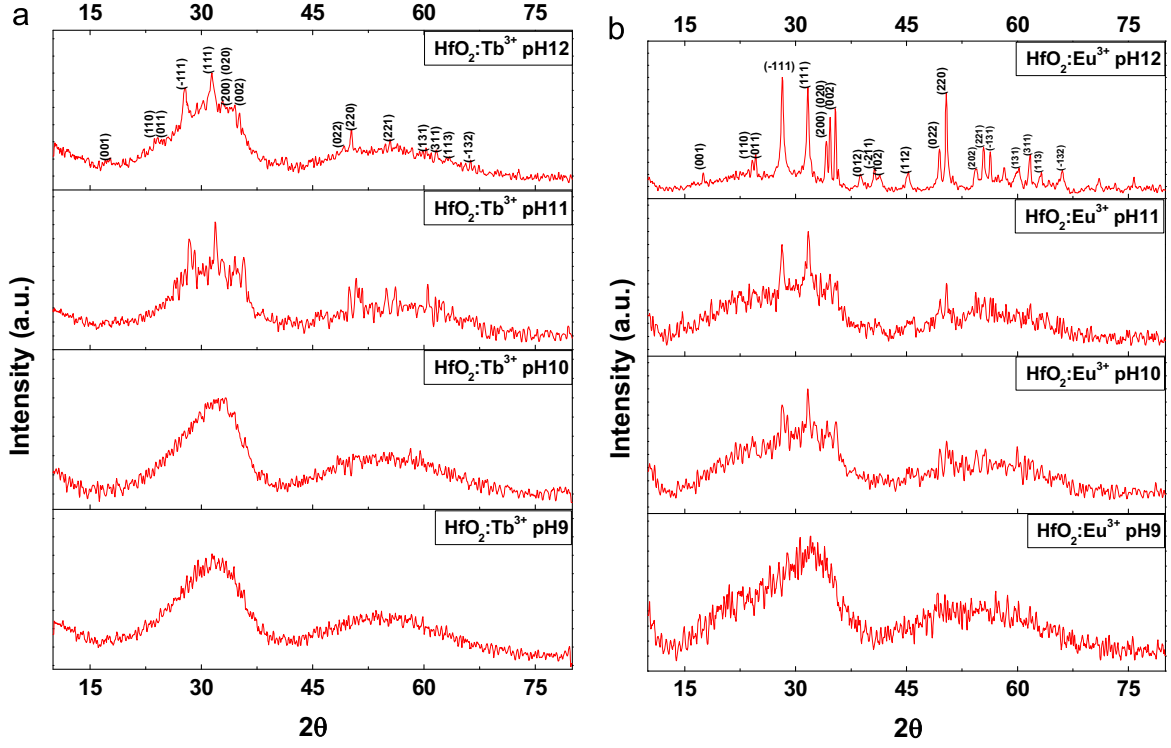

Fig. 1. X-ray diffraction patterns of (a) HfO_2:Tb^{3+}; (b) HfO_2:Eu^{3+} at different values of acidity on the precursor solution.

of 45 nm. From these results, it could be thought that a better crystallinity is obtained when the HfO_2 is doped with Eu^{3+} than the obtained when is dopant with Tb^{3+}, for the same values of acidity. This behavior could be attributed to the difference in the disturbance of the lattice generated by both ions. Although Eu^{3+} ion (0.95 Å) is larger than the Tb^{3+} ion (0.93 Å), the latter seems to have a minor influence on the crystallization of the matrix. This could be due to fact that the distance between europium and its neighbor oxygen (Eu–O ≈ 2.23 Å) is more consistent with the average distance between hafnium and its neighboring oxygen (Hf–O ≈ 2.15 Å), than which has terbium (Tb–O ≈ 2.43 Å) [21–23] which, being greater, could generate a greater distortion in the crystal lattice, inhibiting crystallinity.

Fig. 2a shows the high-resolution scanning micrograph of particles of HfO_2 doped with 3 mol% Tb^{3+}, synthesized a pH=12 in the precursor solution. In the image, it is possible to observe small formations like fibers and spherical shapes with a narrow size distribution. Their rounded shores without well-defined edges, could indicate a low degree of crystallinity of the material, which coincides with the information obtained by X-ray diffraction. Similarly, were obtained micrographs of FESEM of nanoparticles of HfO_2 doped with 3 mol% Eu^{3+} to a pH=12 in the precursor solution (Fig. 2b). The image shows

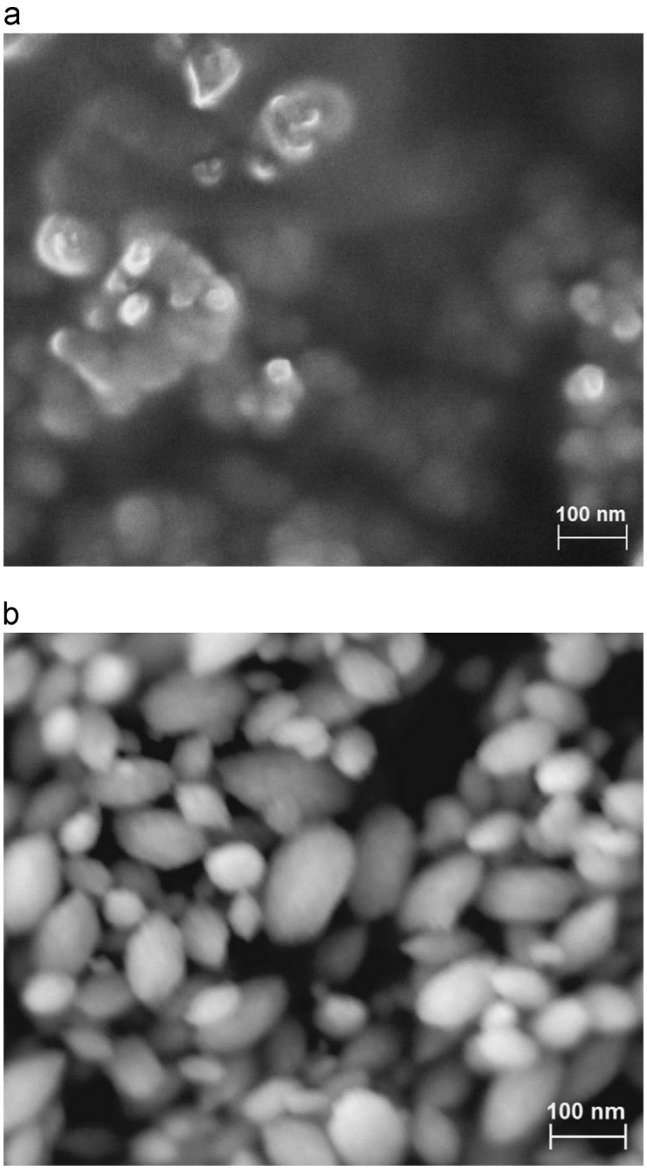

Fig. 2. FESEM micrographs of (a) HfO_2:Tb^{3+} and (b) HfO_2: Eu^{3+}, synthesized to pH=12.

the formation of particles with a relatively wide distribution of sizes, from ~20 nm up to ~110 nm with oval morphology, although it is also possible to observe some particles with prismatic form typical of monoclinic crystals [15]. The contrasting difference in morphology among both samples, suggests that the kinetics of crystallization is affected by the type of dopant, even though they are chemically similar and the difference between their ionic radios it is just of ~0.02 Å.

Table 1 shows the results obtained by EDS, of elements present in the samples of HfO_2 doped with Tb^{3+} (left) and Eu^{3+} (right), synthesized to different degrees of alkalinity in the precursor solution. In both cases it can be seen that the values of oxygen (O), hafnium (Hf), terbium (Tb) and europium (Eu) show little variation with respect to acidity in the precursor solution; however, it is appreciated that stoichiometry relation (O/Hf) is above expectations, could be due to the presence of water molecules trapped in the material due to the high pressure that is exposed during the hydrothermal process [4]. Also, in both cases, the presence of chlorine ions (Cl) was observed, whose concentration had a gradual reduction with increasing alkalinity of solutions. It has been proposed that the incorporation of chlorine ions can be performed by replacing the oxygen in the crystalline lattice [18]. According to the EDS obtained values, seemingly the Tb^{3+} and Eu^{3+} ions are not easily incorporated into the matrix when alkalinity is below pH=6.

Fig. 3 shows the PL emission spectra of HfO2:Tb^{3+}, at different pH levels of the precursor solution, using λ_{ex}=256 nm as wavelength of excitation. The spectra show the characteristic emission lines of the Tb^{3+} transitions; there are four main peaks centered 489 nm, 543 nm, 584 nm and 622 nm that correspond to the transitions $^5D_4 \rightarrow {}^7F_J$ (J=6, 5, 4, 3) respectively, being $^7F_5$ (543 nm) transition of greater intensity and which gives the color green, typical of the Tb^{3+}. An interesting behavior can be observed, since the emission intensity increases of gradual and phased manner in four blocks defined in function of the increase in alkalinity from precursor solutions, (a, b), (c, d, e), (f, g), (h, i). This behavior could be attributed to the fact that, in the hydrothermal condensation process, the formation of hydroxides is the initial state of the process and these are the precursors of the reaction products, i.e., of synthesized oxides. This condensation process is related to the acidity of the solution, which determines the relationship between the number of protons and the number of hydroxides; thereby, the greater the amount of hydroxide in the reaction, the lower the luminescence intensity of condensate, which could explain the behavior observed in the luminescent emission curves. The inset on this figure shows the PL excitation spectrum of the HfO_2 doped with Tb^{3+}, at pH=12 in the precursor solution. The spectrum was obtained using the main emission line centered on 543 nm. It is possible to observe lines of absorption characteristics of trivalent

Table 1
Elements present in (a) HfO_2:$Tb^{3+}$and (b) HfO_2:Eu^{3+}, as a function of precursor solution alkalinity.

(a)					(b)			
Acidity	Concentration (At%) Tb^{3+}				Concentration (At%) Eu^{3+}			
pH	O	Hf	Tb	Cl	O	Hf	Eu	Cl
4	74.3	21.28	0	4.42	70.16	24.03	0	5.81
5	73.85	21.25	0	4.90	71.47	24.1	0	4.43
6	76.07	20.65	0.55	2.73	71.96	24.74	0.26	3.04
7	75.09	22.34	0.39	2.18	74.19	23.02	0.51	2.28
8	76.12	21.23	0.49	2.16	74.8	24.28	0.92	0
9	77.44	21.49	0.64	0.43	75.45	23.73	0.82	0
10	77.59	21.33	0.83	0.25	79.64	19.86	0.50	0
11	78.01	21.63	0.36	0	71.22	27.99	0.79	0
12	77.13	23.27	0.63	0	72.23	26.85	0.92	0

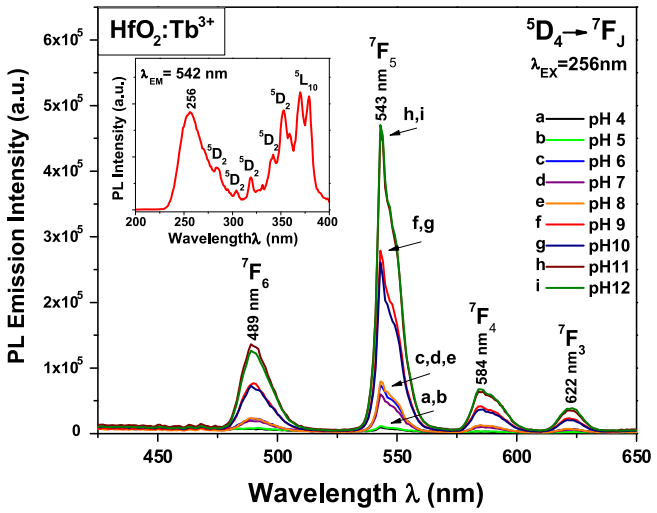

Fig. 3. PL emission spectrum of HfO_2:Tb^{3+}, at different solutions acidity, using an excitation of λ=256 nm. In the inset, the excitation spectrum of HfO_2:Tb^{3+} at pH12, using the emission line $^7F_5$ (542 nm). (For interpretation of the references to color in this figure, the reader is referred to the web version of this article.)

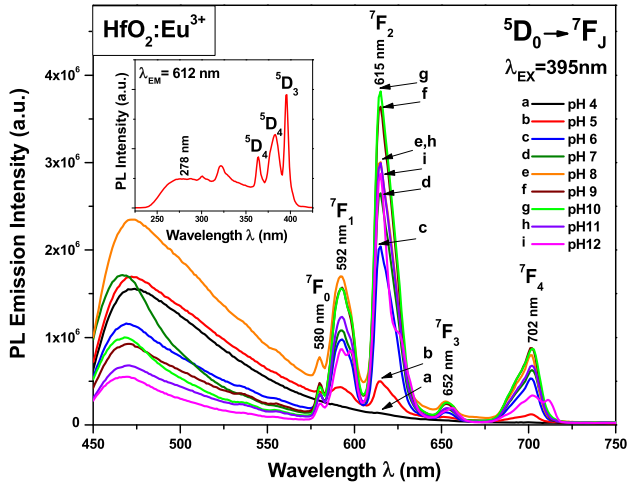

Fig. 4. PL emission spectrum of HfO_2:Eu^{3+}, at different solutions acidity, using an excitation of λ=395 nm. In the inset, the excitation spectrum of HfO_2:Eu^{3+} at pH12, using the emission line $^7F_2$ (612 nm).

terbium above 280 nm, corresponding to the $^5D_2$ and $^5L_{10}$ levels [14]. It can also be seen a broad band in the range between ~230 nm and ~280 nm, centered on 256 nm, which is directly related to 4f–5d transitions of the optically active ions [24]. The comparison between the PL intensities emission of HfO_2:Tb^{3+}using the line $^5L_{10}$ (379 nm) and the wavelength associated with the 4f–5d transitions (256 nm), showed that the latter presents a better optical response, so this wave length was used to carry out all the PL emission spectra of HfO_2:Tb^{3+}. Fig. 4 shows the PL emission spectra of HfO_2:Eu^{3+}, synthesized at different acidity levels of the precursor solution, using λ_{ex}=395 nm as excitation wavelength. The emission spectra show emission lines characteristic of the electronic transitions of Eu^{3+} ion, corresponding to the transitions $^5D_0 \rightarrow {}^7F_J$ (J=0, 1, 2, 3, 4), centered at 580 nm, 592 nm, 615 nm, 652 nm and 702 nm respectively, being the line corresponding to transition $^7F_2$ (615 nm) of greater intensity, which gives the red color, characteristic of the emission in the Eu^{3+}. The behavior in the $^7F_2$ emission line indicates that the intensity increases gradually until reaching a maximum around the pH=10, from which, the emission decreases. This behavior might suggest a change in the local symmetry around the ion, occupying these positions of higher symmetry, which could result in a decrease of the emission intensity.

The inset shows the corresponding excitation spectrum of HfO_2:Eu^{3+}, using a wavelength of 612 nm. Above the 300 nm appear the absorption lines of trivalent europium ^5D_J (J=4, 3), and below this value the band associated with the charge transfer transition between the O^{2-} and optically active ions [13,25,26]. Unlike the case where we used the Tb^{3+} as dopant, in the case of the Eu^{3+} there is an important difference between the intensities of these bands, being the absorption lines belonging to impurity, higher intensity, whose maximum corresponds to the level $^5D_3$ (395 nm); so this wavelength was used to obtain all the emission spectra of the samples doped with Eu^{3+}. Fig. 5 shows the luminescent emission intensity and the percentage of chlorine as a function of pH in the samples doped with Tb^{3+}, reference using the most intense transition ($^5D_4 \rightarrow {}^7F_5$). This graph shows a clearly dependency between the luminescence intensity and the concentration of chlorine ions. It is possible to observe an increase in emission as the concentration of chlorine ions decreases. On the other hand, Fig. 6 shows the luminescent emission intensity and the percentage of chlorine containing as a function of pH in the samples doped with Eu^{3+}, for the $^5D_0 \rightarrow {}^7F_2$ transition. Even though it is not as clear as in the case of the Tb^{3+}, it can be seen a similar behavior, i.e., the intensity increases at smaller concentrations of chloride ions. From our point of view, this behavior is related to the use of the sodium hydroxide (NaOH) for adjust the pH of the precursor solution; since the reaction of sodium hydroxide with salts of starting to give rise to the formation of $M(OH)_N^{\pm Z}$ (M=Hf, Tb, Eu) complexes, besides of sodium chloride (NaCl). Thus the greater the aggregate amount of NaOH solution, the lower the amount of chlorine in the sample, as can be seen in Figs. 5 and 6; however this create a greater amount of $Hf(OH)_N^{\pm Z}$ complexes, as discussed above, these complexes are the precursors of oxide hafnium in the hydrothermal process, which could lead to an increase in the kinetics of crystallization. Having a more crystalline material allows a better distribution of the optically active ions on the material through the crystalline lattice, resulting in a better luminescent emission. It is worth noting that the intersection of curves of luminescent intensity with the percentage of chlorine in Fig. 6, takes place approximately at pH=7, i.e. when the number of ions hydronium (H_3O^+) is almost the same as the number of ions hydroxyl (OH^-) in the solution.

The radiative lifetimes of both dopants, $Tb^{3+}$and Eu^{3+} were determined using the main emission of each ion. In the case of terbium, the analysis was conducted from $^5D_4$ to $^7F_5$ transition centered in 543 nm, using an excitation wavelength of λ_{ex}=489 nm. Fig. 7 shows the decay curves to Tb^{3+}, the curves were fitted with an

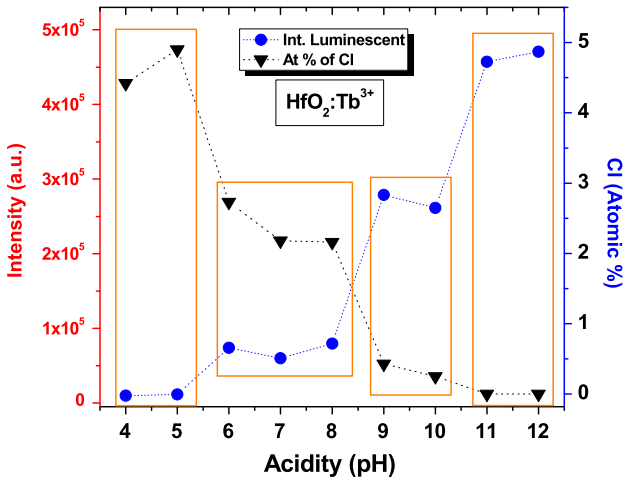

Fig. 5. Relationship between the PL emission intensity and the concentration of chloride ions in HfO_2:Tb^{3+}, as a function of the alkalinity of the precursor solution.

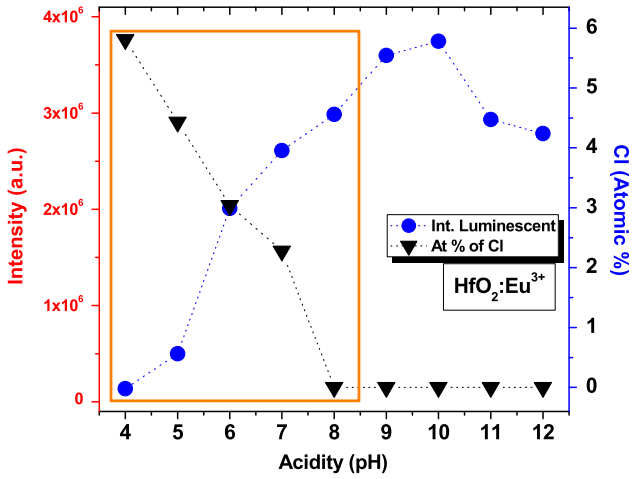

Fig. 6. Relationship between the PL emission intensity and the concentration of chlorine ions in HfO_2:Eu^{3+}, as a function of the alkalinity of the precursor solution.

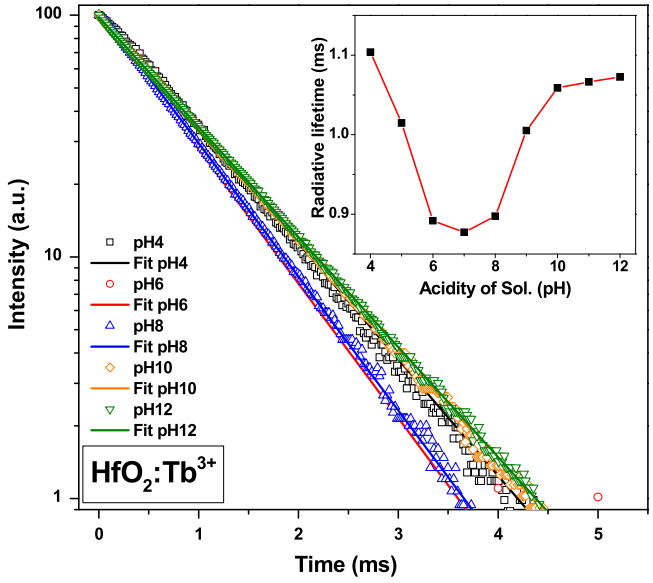

Fig. 7. Emission decay curves of the Tb^{3+} ion. Inset shows the radiative lifetime time from $^5D_4$ to $^7F_5$ transition, as a function of the alkalinity of the precursor solution.

exponential decay function (Eq. (1)).

$$I(t) = Ae^{-t/\tau} \quad (1)$$

where $I(t)$ is the intensity, A is a constant, t is the time and τ is the radiative lifetime. The behavior of τ as a function of pH is seen in the inset. The highest values are in ~1.07 ms for the sample synthesized to pH=12 and ~1.1 ms for the sample synthesized to pH=4. The lowest radiative life was 0.87 ms, obtained at neutral pH. The highest values for τ is found high levels of acidity and alkalinity, which suggests that this behavior could be related to the kinetics of the reaction, due that is obtained a less crystallinity of HfO_2 at neutral pH [16], being able to modify the symmetry around the ion and therefore the radiative lifetime.

The radiative lifetime time for the europium ion was determined from $^5D_0$ to $^7F_2$ transition centered on 614 nm, using an excitation wavelength of 532 nm. Fig. 8 shows the kinetics of the decay curves observed from the hafnium oxide doped with europium. These curves show a slightly deviations from an exponential tendency which suggests the existence of mechanisms of multipolar interaction. Here we use the adjustment proposed by Inokuti–Hirayama (Eq. (2)) [27], which takes into account the nature

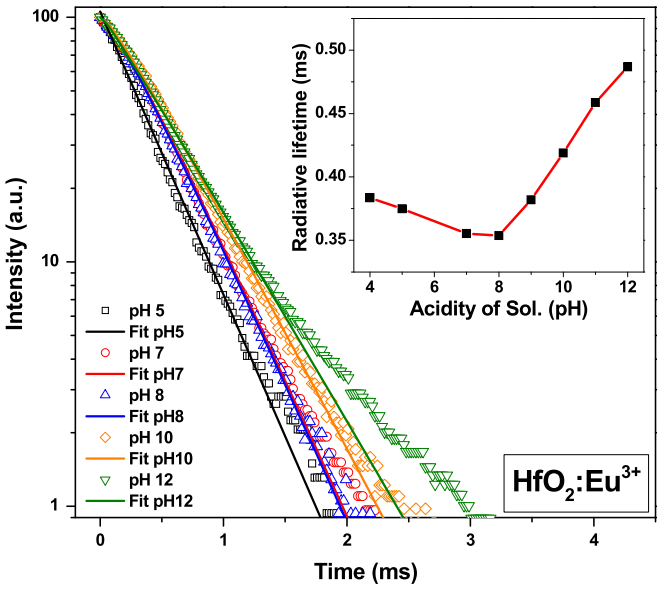

Fig. 8. Emission decay curves of the Eu^{3+} ion. Inset shows the radiative lifetime time from $^5D_0$ to $^7F_2$ transition, as a function of the alkalinity of the precursor solution.

of the transition.

$$I(t) = I(0)e^{\left(-(t/\tau)-\left(Q(t/\tau)^{3/S}\right)\right)} \quad (2)$$

where I is the spectral intensity, Q involves the acceptor–donator concentration as well as the probability of energy transfer in addition the Γ function, while S factor involves the nature of the transition, and can take values of 6 (dipole–dipole), 8 (dipole–quadrupole), 10 (quadrupole–quadrupole) [28]; the best fitting was obtained with the factor $S=6$. Inset shows the behavior of τ as a function of pH, being observed a shortest decay time at neutral pH environment besides of an increase in τ when alkaline values increases. The lifetime time of this ion takes values of ~350 μs at pH=8 and a near maximum of ~490 μs to pH=12, i.e. three orders of magnitude lower than those obtained for the Tb^{3+} ion. The behavior of the maxima and minima in the radiative lifetime of the Eu^{3+} is similar to that found for the Tb^{3+}, and also indicates a possible dependence of this with the local symmetry and the kinetics of the reaction of the HfO_2.

4. Conclusions

The analysis of data obtained, suggest the existence of a close relationship between the acidity of the precursor solution and the structural and luminescent properties of the HfO_2:Ln^{3+}. By increasing the alkalinity in the precursor solution, is notorious an increase in the kinetics of the reaction, thus promoting a better crystallinity; however, this increase is not the same for both ions, the X-ray diffraction patterns and SEM micrographs show that the material doped with Eu^{3+} ions presents greater reaction kinetics, resulting in larger and more defined crystals. Equally clearly, the correlation between the intensity of luminescent emission with the concentration of chlorine ions, which in turn is closely related to the pH of the precursor solution, being the Tb^{3+} ion the most affected by the inhibitory effect of chloride ions, as far as we know, this is one of the few works that attempt to clarify this behavior. On the other hand, although the decay kinetics behavior is similar for both ions, only europium presents a multipolar interaction.

Acknowledgments

We thank the Consejo Nacional de Ciencia y Tecnología (CONACyT) and SIP-IPN for the financial support through the program No. 20150189.

References

[1] E. Villanueva-Ibañez, C. Le Luyer, O. Marty, J. Mugnier, Opt. Mater. 24 (2013) 51.
[2] A.I. Ramos-Guerra, J. Guzmán-Mendoza, M. García-Hipólito, O. Alvarez-Fregoso, C. Falcony, Ceram. Int. 41 (9, Part A) (2015) 11279.
[3] R.-J. Xie, N. Hirosaki, Sci. Technol. Adv. Mater. 8 (2007) 588.
[4] E. Montes, P. Cerón, T. Rivera Montalvo, J. Guzmán, M. García-Hipólito, A. B. Soto-Guzmán, R. García-Salcedo, C. Falcony, Appl. Radiat. Isot. 83 (2014) 196.
[5] G.C. Tyrrell, Nucl. Instrum. Methods Phys. Res. A 546 (2005) 180.
[6] L. Martínez Maestro, P. Haro-González, M.C. Iglesias-de la Cruz, F. Sanz-Rodríguez, Á. Juarranz, J. García Solé, D. Jaque, Nanomedicine 8 (3) (2013) 379.
[7] S. Lange, V. Kiisk, V. Reedo, M. Kirm, J. Aarik, I. Sildos, Opt. Mater. 28 (2006) 1238.
[8] J.M. Léger, J. Haines, B. Blanzat, J. Mater. Sci. Lett. 13 (23) (1994) 1688.
[9] A. Wiatrowska, E. Zych, L. Kępiński, Radiat. Meas. 45 (2010) 493.
[10] G. Štefanić, S. Musić, K. Molčanov, J. Alloy. Compd. 387 (2005) 300.
[11] M. Vargas, N.R. Murphy, C.V. Ramana, Opt. Mater. 37 (2014) 621.
[12] J.P. Lehan, Y. Mao, B.G. Bovard, H.A. Macleod, Thin Solid Films 203 (2) (1991) 227.
[13] C. Chacón-Roa, J. Guzmán-Mendoza, M. Aguilar-Frutis, M. García-Hipólito, O. Alvarez-Fragoso, C. Falcony, J. Phys. D: Appl. Phys. 41 (2008) 015104.
[14] G.H. Dieke, Spectra and Energy Levels of Rare Earth Ions in Crystals, Interscience Publishers, USA, 1968.
[15] E. Navarro Cerón, G. Rodríguez Gattorno, J. Guzmán, M. García-Hipólito, C. Falcony, Open J. Synth. Theory Appl. 2 (2013) 73.
[16] G. Štefanić, K. Molčanov, S. Musić, Mater. Chem. Phys. 90 (2005) 344.
[17] X. Lu, C. Chen, S. Husurianto, M.D. Koretsky, J. Appl. Phys. 85 (8) (1999) 4154.
[18] Y. Shimomura, N. Kijima, J. Electrochem. Soc. 151 (8) (2004) H192.
[19] J.C. Alonso, E. Haro-Poniatowski, R. Diamant, M. Fernandez-Guasti, M. García, Thin Films Solids 303 (1–2) (1997) 76.
[20] B.D. Cullity, S.R. Stock, Elements of X-Ray Diffraction, Prentice Hall, New Jersey, USA (2001), p. 170.
[21] W.H. Zachariasen, Norsk Geologisk Tidsskrift 9 (1927) 310.
[22] R. Ruh, P.W.R. Corfield, J. Am. Ceram. Soc. 53 (1970) 126.
[23] E. Hubbert-Paletta, H.K. Mueller-Buschbaum, Z. fuer Anorg. und Allg. Chem. 363 (1968) 145.
[24] G. Blasse, B.C. Grabmaier, Luminescent Materials, Springer-Verlag, Germany, 1994.
[25] R. Chora-Corella, M. García-Hipolito, O. Álvarez-Fragoso, M.A. Álvarez-Pérez, C. Falcony, Rev. Mex. de Fís. 55 (3) (2009) 226.
[26] A. Huignard, T. Gacoin, J.P. Boilot, Chem. Mater. 12 (2000) 1090.
[27] M. Inokuti, F. Hirayama, J. Chem. Phys. 43 (1965) 1978.
[28] I.R. Martin, Transferencia de Energía entre Iones 4f en Vidrios Fluorindatos. Tesis Doctoral, Spain, 1996.